

TEMPORAL RESOLUTION IN OLFACTION: STIMULUS INTEGRATION TIME OF LOBSTER CHEMORECEPTOR CELLS

GEORGE GOMEZ* AND JELLE ATEMA†

Boston University Marine Program, Marine Biological Laboratory, Woods Hole, MA 025431, USA

Accepted 29 April 1996

Summary

The stimulus integration time of lobster olfactory receptor cells *in situ* was determined using extracellularly recorded spiking responses from receptor cells and on-line high-resolution measurement of odor square pulses. At a fixed odor concentration, odor steps of 200 ms duration elicited maximum responses; shorter odor steps did not drive the cells to their maximum response and longer odor steps added spikes but did not result in higher firing rates. Excitatory processes peaked within 220 ms of stimulus onset. At 160–300 ms, stimulus intensity discrimination was most evident. Adaptation processes reduced response magnitude to near-zero levels within 1000 ms of stimulus

onset. Olfactory receptor cells thus resolve odor peak onsets within the first few hundred milliseconds: this time window corresponds to the 4–5 Hz frequency of olfactory sampling (i.e. ‘sniffing’) as well as the rapid fluctuations in odor concentration that are common in natural odor plumes. The stimulus integration time of 200 ms may play a role in the filtering of information used by lobsters to orient to distant odor sources.

Key words: olfaction, crustacean, filter properties, electrophysiology, chemoreception, lobster, *Homarus americanus*.

Introduction

Recent investigations of the kinetics of olfaction have shown that olfactory systems are capable of resolving rapid events. Second messenger production *in vitro* and receptor potential generation in isolated olfactory receptor neurons occur within 100 ms of stimulus onset. However, little is known about the temporal capabilities of chemoreceptor systems *in situ*, probably in part because of the lack of accurate stimulus quantification methods. Most research in chemoreception has focused on the decoding of complex mixtures, with little attention to stimulus dynamics. Yet it has been suggested that animals such as moths (Murlis *et al.* 1992; Kaissling and Kramer, 1990), lobsters (Atema, 1985, 1988; Moore *et al.* 1991b) and crabs (Weissburg and Zimmer-Faust, 1993; Zimmer-Faust *et al.* 1995) may use the temporal information present in the dynamic fluctuations in an odor plume to derive useful directional and distance information regarding the odor source. Behaviorally, moths have been shown to respond to changes in the odor environment within 300 ms (Vickers and Baker, 1994; Mafra-Neto and Cardé, 1994). Lobsters appear to make behavioral chemotactic decisions within 2 s (Basil *et al.* 1995). Humans discriminate olfactory (Laing and MacLeod, 1992) and taste (Lester and Halpern, 1979) information within 680 and 400 ms, respectively.

To determine the range of odor fluctuations to which animals respond, we must know the temporal resolution of peripheral

chemoreceptor cells. An important parameter that determines temporal resolution is the stimulus integration time of the receptor cells, or the minimum time it takes for a receptor cell to measure the stimulus intensity of a stimulus pulse (Hood and Grover, 1974; Duysens *et al.* 1991; Firestein *et al.* 1990). To determine the temporal resolution limits of the visual system, various investigators have measured the integration time of photoreceptors and other retinal components. Photoreceptor cell responses to brief flashes of light depend on total stimulus energy within a ‘critical time’ period of about 100 ms; light intensity and duration are interchangeable within this time period (Barlow, 1958; Hood and Grover, 1974). Beyond the critical time, responses are dependent primarily on stimulus intensity. This physiological property is reflected in the psychophysical capabilities of the visual system: when given brief flashes of light of equal energy, stimulus duration and intensity are again interchangeable; thus, brief flashes of light appear dimmer. This relationship, known as Bloch’s law, specifies the lower limit for the accurate determination of light intensity as the critical time (Levick and Zacks, 1970; Duysens *et al.* 1991).

In this study, we determined the integration time of olfactory receptor neurons from the lateral antennule (the appendage known to mediate distance orientation; Devine and Atema, 1982) of the American lobster *Homarus americanus*. The

*Present address: Monell Chemical Senses Center, 3500 Market Street, Philadelphia, PA 191042, USA.

†Author for correspondence.

amino acid trans-4-hydroxy-L-proline (Hyp) excites a large proportion of chemoreceptors on the antennule (Johnson and Atema, 1983) and was thus used as the odor stimulus. We used rapid *in situ* stimulation and high-resolution stimulus measurement (Gomez *et al.* 1994) to ensure accurate stimulus control. We first determined whether odor steps of equal volume produced a similar response – that is, whether a short step at a high concentration and a longer pulse at a lower concentration were indistinguishable to the cell (Bloch's law). Then we set out to determine the time range over which Bloch's law would apply and to determine the time period over which receptor cells would 'count' stimulus molecules to encode the stimulus concentration of the odor step.

Materials and methods

Experimental procedure

Lateral antennules from intermolt lobsters *Homarus americanus* L. were excised and prepared as described previously (Gomez *et al.* 1992, 1994). Briefly, antennules were dissected to expose the axon bundles of the olfactory receptor neurons and placed in an olfactometer. Receptor cell responses were recorded extracellularly. For controlled stimulus delivery, we employed a focal stimulation technique with pressurized concentric pipettes that allowed the rapid introduction and removal of stimulus solutions to and from the aesthetasc (olfactory) sensilla. These sensilla contain the dendritic regions of the olfactory receptor neurons. To verify each stimulus presentation, we monitored tracer molecule (dopamine mixed with the stimulus solution) concentrations on-line in the area of stimulus delivery using a high-resolution (5 ms temporal, 30 μm spatial) electrochemical detector (IVEC-5, Medical Systems Corp.). Hyp-sensitive olfactory neurons were identified with 50 μl samples of 100 $\mu\text{mol l}^{-1}$ Hyp introduced into a 30 ml min^{-1} superfusion of artificial sea water. The responsive receptor cell was then localized to within one antennule segment using 10 $\mu\text{mol l}^{-1}$ odor pulses from the stimulus pipettes. Receptor cells were then stimulated with odor steps of 50, 100, 200, 500 and 1000 ms, each at 1, 5, 10, 50 and 100 $\mu\text{mol l}^{-1}$ Hyp. A computer-generated trigger pulse initiated the stimulus delivery and synchronized the IVEC and electrophysiological recordings. Each stimulus presentation was repeated at least three times. The order of presentation of the different odor step lengths at one stimulus concentration was randomized. If the on-line stimulus recording showed that the odor step was not as 'square' as intended (i.e. the peak level of the step varied by over 10 %), the step was repeated. At least 1 min separated each stimulus presentation. When the odor steps at one concentration were all delivered, the stimulus solution in the delivery system was completely purged and replaced with a solution at another concentration without moving the stimulus pipettes. The preparation was then allowed to remain undisturbed for at least 3 min. There was no spontaneous spike activity for at least 10 s prior to the presentation of each odor step.

Data analysis

Only data from cells that completed all three repetitions of all five odor steps at all five concentrations were analyzed. Odor steps were quantified as follows: onset time was the time from the first data point above the noise level to the time that 80 % maximum step amplitude was attained; offset time was the time from the initial decline of the stimulus to the time that the step amplitude had dropped by 80 %; step length was the time from the end of the stimulus onset to the start of the stimulus offset; step amplitude was the maximum concentration measured within a step. To quantify total stimulus delivered (for data shown in Fig. 3), we measured the area under the intensity–time curve for each odor step.

Since the start of stimulus onset times (measured by IVEC) typically occurred within 5 ms (one data point) of the start of the trigger pulse, the time of occurrence of each spike was measured from the start of the trigger. For each odor step, we only considered the spikes occurring within 1.5 s from the start of the stimulus trigger; this period seemed adequate to measure the chemoreceptor response since these receptor cells displayed little or no spontaneous activity and responded with brief spike bursts that usually terminated within 1 s. For each odor step, we quantified the following response parameters: the number of spikes was the total number of spikes that occurred within the 1.5 s response window; first spike latency was defined as the time from the onset of the trigger pulse to the time of occurrence of the first spike; the instantaneous frequency along the response was computed as the inverse of each interspike interval (in s); maximum number of spikes in 100 ms was defined as the highest number of spikes that occurred in any 100 ms time period within the response. Mean number of spikes (see Fig. 5) and mean first spike latency (see Fig. 6) of the population were computed by averaging the values generated by each receptor cell to three repetitions of an odor step.

Peri-stimulus time histograms depict the population response by combining the responses of one repetition from all receptor cells. The response was then divided into 20 ms time bins and the total number of spikes within each 20 ms bin was counted. For clarity of presentation, the curves of the peri-stimulus time histograms were smoothed using a natural spline function (PSI Plot, Poly Software International).

For descriptive simplicity, odor step amplitudes and lengths are referred to as the pipette stimulus concentration and the duration of the trigger pulse, respectively. Actual stimulus values are reported in the results. Values are reported as mean \pm standard deviation (S.D.) unless otherwise noted. Pilot experiments showed that steps shorter than 50 ms could result in the step not reaching full amplitude and thus were not used in this study.

Results

Fourteen receptor cells completed the entire stimulus protocol in good health and were used for data analysis.

Single cell responses: sample cells

The stimulation apparatus and on-line stimulus measurement allowed us to deliver replicable odor steps with a rapid onset and removal of odor molecules into and away from chemoreceptor sensilla. Fig. 1A shows an example of the measured stimulus (upper trace) and the corresponding spike events (lower trace) generated by a single receptor cell. Here, the stimulus was turned on at $t=0$ and turned off at $t=1$ s. The onset and offset slope times were 25 ms each; step length was 1000 ms, step amplitude was $99\ \mu\text{mol l}^{-1}$. The stimulus trace shows a typical odor step obtained with each stimulus presentation; steps that deviated from this general form were rejected on-line and repeated with improved stimulus conditions. Fig. 1B shows an example of the replicability of odor step amplitudes of different pulse lengths for one experiment. The measured values for the onset and offset times for all the odor steps used in the experiments were 35 ± 18 ms and 75 ± 38 ms, respectively. Mean odor step lengths reported and, in parentheses, the actual values measured in ms were as follows: 50 (38 ± 11), 100 (88 ± 27), 200 (176 ± 44), 500 (471 ± 87) and 1000 (962 ± 103); no step length varied by more than an average of 7%. The mean odor step amplitudes

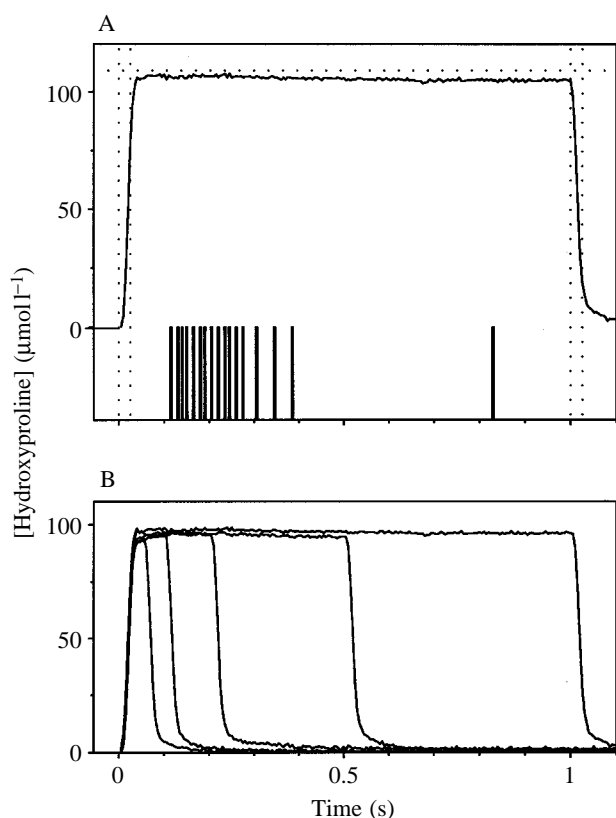


Fig. 1. (A) Sample odor step used in the experiment (upper trace) and corresponding spike events recorded from a single receptor cell (lower trace). Dotted lines show times of onset slope, peak level and times of offset slope of the odor step. (B) Odor steps of 50, 100, 200, 500 and 1000 ms at $100\ \mu\text{mol l}^{-1}$ hydroxyproline attained the intended peak amplitude with identical onset slopes and little variability in mean duration ($<7\%$).

reported (and measured) were (in $\mu\text{mol l}^{-1}$) 1 (0.97 ± 0.08), 5 (4.6 ± 0.64), 10 (9.3 ± 1.1), 50 (47.5 ± 7.12) and 100 (94.9 ± 11.8); no amplitude varied by more than an average of 20%. Thus, under the conditions of our experiments, there was essentially little dilution of the stimulus solutions from the pipettes to the preparation.

Spike responses were typically phasic bursts with little or no tonic activity. Responses often terminated even if odor was still present. First spike latency of the response seen in Fig. 1A was 113 ms. The maximum instantaneous spike frequency observed in this response was 88 Hz, occurring after the third spike.

Fig. 2 shows a characteristic response matrix of a single cell to one repetition of all odor steps used. The maximum spike frequency generated by this receptor cell was 114 Hz (fourth spike in the response to the 50 ms $100\ \mu\text{mol l}^{-1}$ step). At the two lowest stimulus concentrations, the cell responded with low-frequency spike activity only after being stimulated for 200 ms. Apparently, odor encounters were integrated over this time period to reach firing threshold. Odor steps of increasing concentration resulted in more spikes, higher spike frequency and shorter response latency. Longer odor steps resulted in a longer response duration. Responses were phasic: short (50–200 ms) odor steps resulted in a brief burst of spike activity lasting 100–200 ms. Longer odor steps resulted in a 100–200 ms phasic burst followed by a continuous decline of spike activity, usually terminating before the odor pulse was turned off. Higher step amplitudes resulted in a more phasic response with less of a tonic portion. The stimulus–response characteristics reported for this cell were representative of all the cells studied.

To determine whether receptor cell responses depended on total number of molecules encountered, we compared responses to odor steps that delivered a similar number of molecules near the receptor surface over different periods. Expressing the delivered stimulus as a liquid volume is inappropriate since chemoreceptor cells do not measure volumes; they measure molecular encounters. Since the *in situ* stimulus measurement with IVEC measures molecular encounters of the tracer (Gerhardt *et al.* 1982), we used the area under the measured stimulus curve (the ‘molar–time product’) as a metric for molecular density over time. For example, the odor step shown in Fig. 1 had a total area of $97\ \mu\text{mol l}^{-1}\text{ s}$.

Fig. 3 shows responses of a single cell to odor steps that delivered the same molar–time product ($9.7\pm 1.1\ \mu\text{mol l}^{-1}\text{ s}$) over three different time periods. In each case, stimulus onset is at $t=0$. The patterns of spike responses were related to odor step amplitude and not to total stimulus delivered: higher odor steps resulted in shorter latencies, both to first spike and to maximum firing frequency, as well as higher spike numbers and frequencies. This was true for all receptor cells studied. For these cells at these odor step amplitudes and times, Bloch’s law did not apply. It is possible that receptor cells encode the total number of stimulus molecules *per se* over shorter time intervals than those used in this study.

The stimulus integration time of a receptor cell may be described as the minimum length of an odor step eliciting the

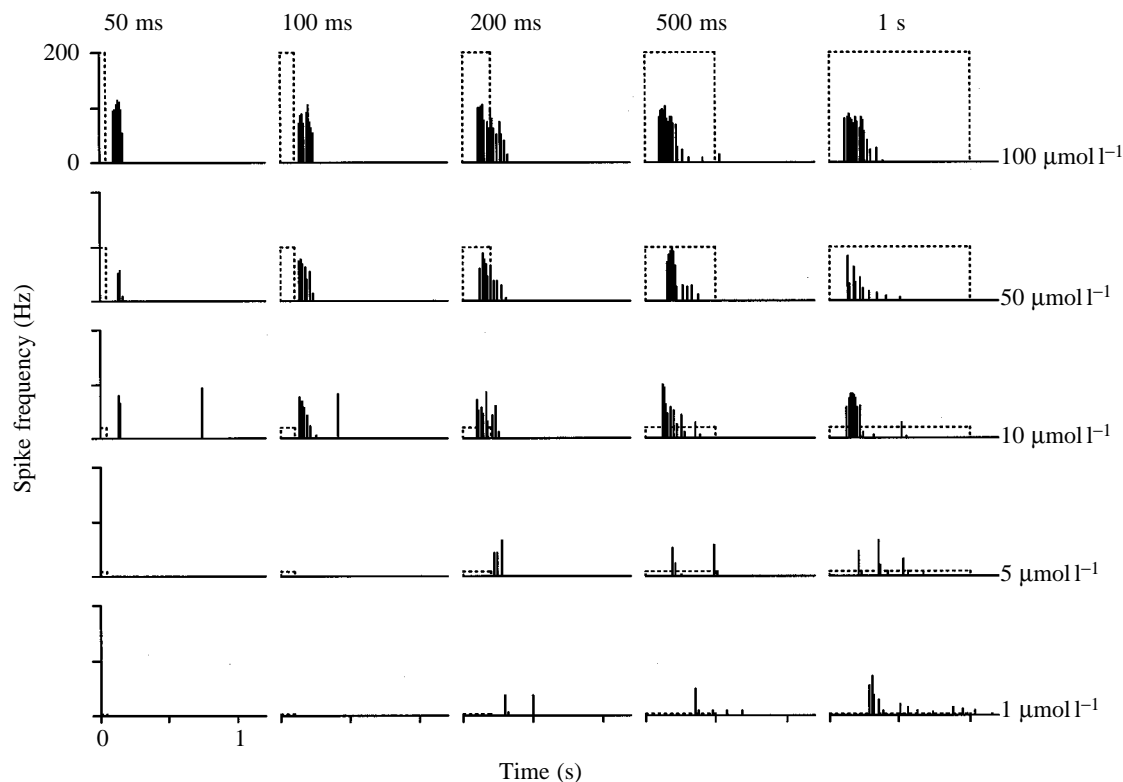


Fig. 2. Responses of a representative single cell (instantaneous spike frequency) to a stimulus matrix: 50, 100, 200, 500 and 1000 ms steps of hydroxyproline each at 1, 5, 10, 50 and $100 \mu\text{mol l}^{-1}$. Dotted boxes represent the odor steps delivered to the cell.

'maximum response' for that step amplitude. To quantify this maximum response, we measured both the maximum instantaneous spike frequency and the maximum number of spikes in any 100 ms time period of the response; the latter gave a good estimate of the average firing frequency during the cell's phasic spike activity. In most cases, the 100 ms time bin with the maximum number of spikes started at spikes 1–3 of

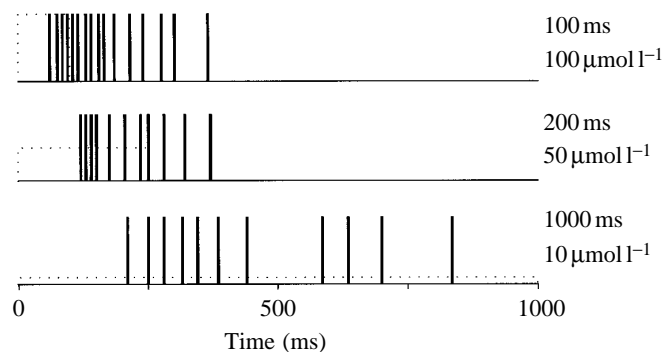


Fig. 3. Spike responses of a single cell to three odor steps that delivered the same 'molar-time product' ($9.7 \pm 1.1 \mu\text{mol l}^{-1} \text{ s}$) over different time periods. Dotted boxes represent the odor steps delivered to the cell, and odor step lengths and amplitudes are indicated to the right of each spike train. Responses to a 100 ms $100 \mu\text{mol l}^{-1}$ odor step had a total number of 16 spikes, a first spike latency of 59 ms and a maximum spike frequency of 110 Hz (fourth spike). Responses of the same cell to a 200 ms $50 \mu\text{mol l}^{-1}$ odor step had a total of 16 spikes, a latency of 117 ms and a maximum frequency of 103 Hz (third spike). Responses of the cell to a 1000 ms $10 \mu\text{mol l}^{-1}$ odor step had a total of 11 spikes, a latency of 207 ms and a maximum frequency of 35 Hz (fourth spike).

the response. Fig. 4 shows the maximum response values for the responses of the cell shown in Fig. 2. Values were averaged over three repetitions of each odor step. At the lowest odor step amplitude ($1 \mu\text{mol l}^{-1}$), step lengths of 50 and 100 ms failed to elicit a spike response. At this amplitude, steps of 200 ms resulted in a maximum response of 40 Hz and 2.5 spikes in 100 ms; these values did not increase significantly with longer odor steps. At the step amplitude of $5 \mu\text{mol l}^{-1}$, 50 ms steps failed to elicit a spike response and 100 ms steps elicited 1 spike. Steps of 200 ms and longer resulted in a similar maximum response to odor steps of $1 \mu\text{mol l}^{-1}$. At the step amplitudes of 10 and $50 \mu\text{mol l}^{-1}$, spike responses started with 50 ms odor steps and attained their maximum response values with steps of 200 ms and longer. Responses to 10 and $50 \mu\text{mol l}^{-1}$ steps were each significantly greater than responses to 1 or $5 \mu\text{mol l}^{-1}$ steps ($P < 0.05$, ANOVA). At $100 \mu\text{mol l}^{-1}$ step amplitude, cell responses attained their maximum frequency (113 Hz) with the shortest odor step (50 ms). Longer odor steps did not result in an increase in maximum frequency, but did result in a higher number of spikes in 100 ms, reaching a peak with 200 ms odor steps. Thus, for this single cell, the stimulus integration time was 200 ms regardless of odor concentration. A similar value for integration time was obtained for 12 of the 14 receptor cells tested.

Population responses

Mean population responses showed that both increased odor step amplitude and increased step length resulted in increased spike numbers (Fig. 5). Response latencies varied greatly between cells and concentrations. As expected, odor step

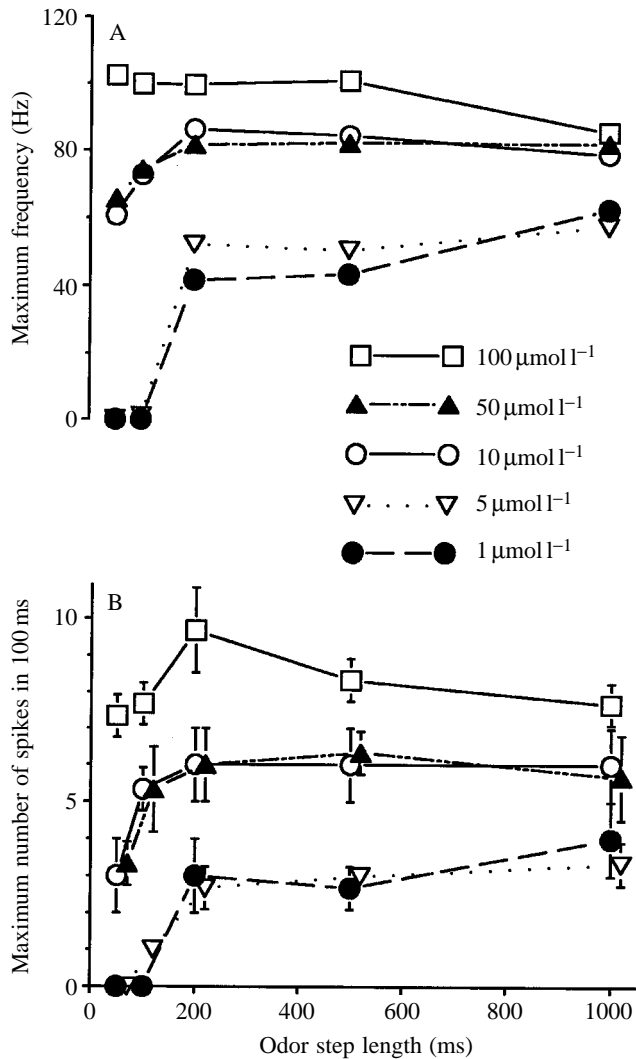


Fig. 4. The 'maximum response' for the single cell shown in Fig. 2 given as both the maximum instantaneous spike frequency (A) and the maximum number of spikes in any 100 ms period (\pm S.D.) (B). Lines connect responses to different odor step lengths at the same step amplitude. Data points in each graph show the mean for three replicates of each stimulus application. Error bars in A were omitted for clarity; the largest variance observed for this graph was 27%. In B, data points are offset on the x-axis to show error bars clearly.

lengths at any one concentration had no significant effect on first spike latency ($P \gg 0.1$, ANOVA). However, increased odor concentration resulted in significantly decreased first spike latency ($P < 0.01$, F -test; Fig. 6). This was computed using the mean latency of the responses to different odor steps regardless of step lengths. The shortest latency value measured was 41 ms (50 ms step length, 100 $\mu\text{mol l}^{-1}$ step amplitude) while the longest latency value measured was 1376 ms (50 ms step length, 1 $\mu\text{mol l}^{-1}$ step amplitude); it may be coincidence that both extremes occurred at 50 ms step lengths. Latency variance was greater with 1 $\mu\text{mol l}^{-1}$ steps than with 100 $\mu\text{mol l}^{-1}$ steps.

To quantify the integration time of the receptor cell population as a whole, peri-stimulus time histograms were

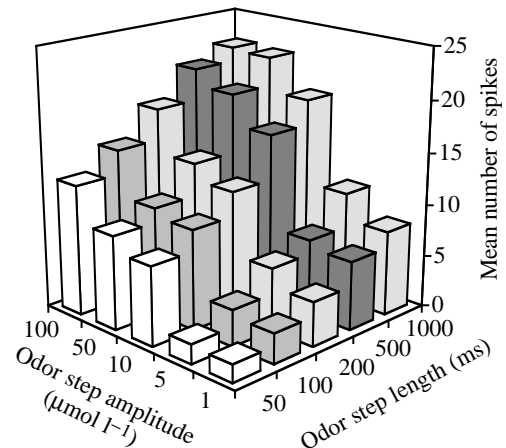


Fig. 5. Mean number of spikes of all 14 cells generated in response to each of three replicates of an odor step.

constructed as described in Materials and methods. As with the single cell records, we determined for each concentration the minimum step length that elicited the maximum response (here defined as the highest number of spikes in 20 ms) from the summed receptor cell spike activity (Fig. 7). At the lowest odor step amplitude (1 $\mu\text{mol l}^{-1}$; Fig. 7, bottom graph), a 50 ms step resulted in a response that peaked to 5 spikes per 20 ms at approximately 160 ms and lasted for 300 ms. A 100 ms step resulted in a higher peak response (8 spikes per 20 ms) at approximately 180 ms. Longer odor steps (200, 500 and 1000 ms) resulted in comparable peak responses (10–11 spikes per 20 ms) at approximately 200–220 ms. (Note: the transient increase in activity of the response to the 200 ms step at 700 ms is an artifact of the smoothing algorithm.) Thus, at this lowest odor step amplitude, step lengths of 200 ms resulted in the response attaining a maximum value; steps longer than 200 ms

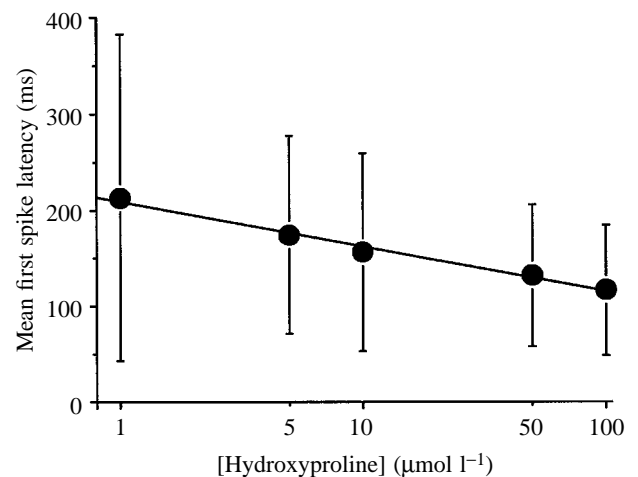


Fig. 6. Mean \pm S.D. first spike latencies of responses to odor steps at each concentration plotted against odor step concentration. Since odor step length had no significant effect on first spike latency ($P \gg 0.1$, ANOVA), latency values for responses to all step lengths at one step amplitude were averaged. Latency varied linearly ($r^2 = 0.99$) with the logarithm of step amplitude (F -test, $P < 0.01$).

did not significantly drive the response any further, and steps shorter than 200 ms did not result in the response attaining a maximum value (Welsch step-up procedure: $\alpha=0.05$, d.f.=13, Sokal and Rohlf, 1981). After attaining the maximum value, spike numbers declined even if the stimulus was still present. Longer odor steps resulted in a more gradual decline to baseline levels. Higher odor step concentrations resulted in an increased spike activity (note different y-axis values in Fig. 7). However, at all but the highest concentration, odor steps of 200 ms and longer resulted in a maximum response. At $100 \mu\text{mol l}^{-1}$ step amplitude, the maximum response was attained with a 100 ms pulse (Welsch step-up procedure, Sokal and Rohlf, 1981); thus, at this step amplitude, the population integration time was 100 ms.

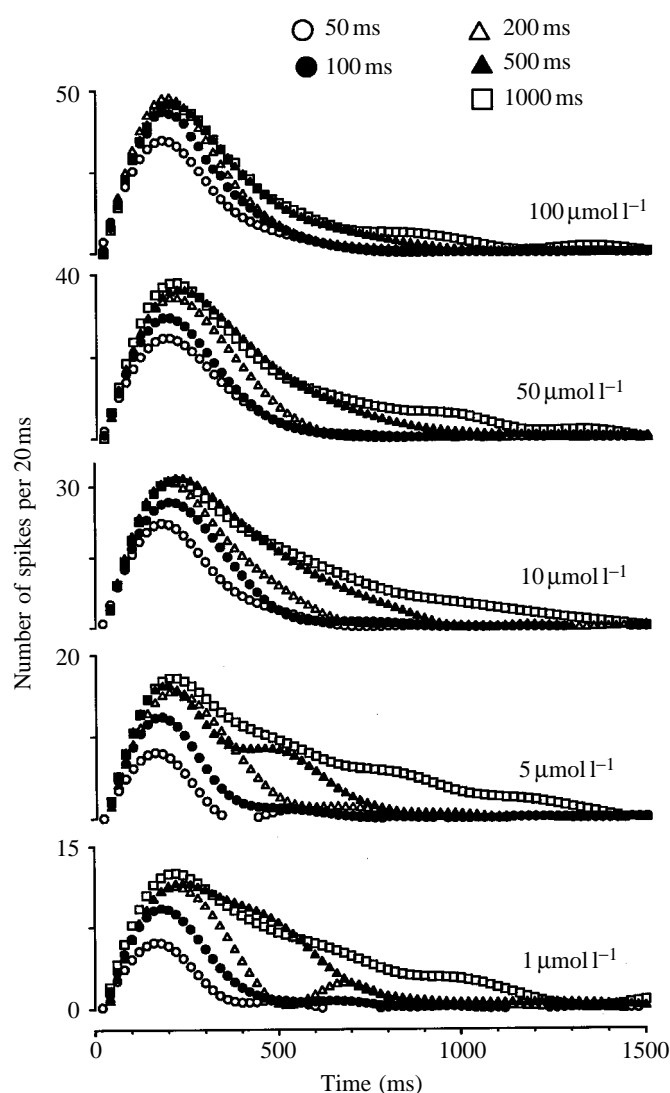


Fig. 7. Population responses to different odor step lengths at the same step amplitude. Responses of all 14 receptor cells to one replicate of each odor step were summed and grouped into 20 ms time bins (peristimulus time histograms). The curves were smoothed using a natural spline function for clarity and ease of comparison. Note that the y-axis is different for each graph, reflecting the increase in response magnitude with increasing step amplitude.

To quantify the intrapulse adaptation characteristics of the receptor cell population, cell responses to odor steps of a fixed length at different concentrations were compared (Fig. 8). Responses were quantified as in Fig. 7. Odor step lengths of 1 s (Fig. 8, top graph) resulted in spike activity that attained maximum values at 180–220 ms. These periods of maximum activity were rarely sustained despite the ongoing presence of the stimulus: immediately following the peak in activity, the spike response declined to half peak-amplitude at 420–600 ms and returned to zero within 1.5 s. Shorter odor step lengths (50, 100, 200 and 500 ms) also resulted in spike activity that peaked at 180–220 ms. With 500 ms odor steps, responses declined to half peak-amplitude at 420–580 ms and to zero within 1.2 s. With 200 ms odor steps, responses declined to half peak-amplitude within 380–420 ms and to zero within 1 s. With 100 ms odor steps, responses declined to half peak-amplitude within 300–380 ms and declined to zero within 700 ms. With 50 ms odor steps, responses declined to half peak-amplitude within 280–360 ms and to zero within 700 ms. Thus, even with the stimulus present, spike responses declined to a point where there was no difference in spike activity between responses to different step amplitudes. For example, with 1 s steps, responses to step amplitudes of 10, 50 and $100 \mu\text{mol l}^{-1}$ were indistinguishable after 500 ms; responses to all five step amplitudes were indistinguishable after 800 ms.

To summarize, the time course of response onset is determined only by odor step amplitude; response offset and return to zero baseline are functions of step length. The concentration–response function was thus most evident around 200 ms following stimulus onset, with curiously little difference between 1 and $5 \mu\text{mol l}^{-1}$ and between 10 and $50 \mu\text{mol l}^{-1}$ steps. Stimulus duration appeared to be somewhat reflected in ongoing very infrequent firing.

Discussion

The results demonstrate that these lobster olfactory receptor neurons responded primarily to the first 200 ms of odor steps and integrated stimuli over that period. Increased odor step amplitude caused greater spike activity (Fig. 5), shorter first spike latency and smaller latency variance (Fig. 6), but did not affect the time to peak response (Fig. 8). Differences in spike activity were most evident at 200 ms following stimulus onset, thus providing optimal stimulus intensity discrimination at that time (Fig. 8). An earlier study on antennular Hyp cells in lobster showed that intensity discrimination became optimal at 250 ms response duration, while longer responses did not change discriminability (Johnson *et al.* 1991). The integration and adaptation time courses of these receptor cell responses result from rapid cellular transduction processes and imply that these cells may be optimized to filter specific transient events from natural odor environments: the 200 ms peak discrimination window implies a rather narrow optimal 5 Hz frequency filter for this cell population (Gomez *et al.* 1994).

Studies on the kinetics of transduction cascades in olfactory receptor neurons (Breer *et al.* 1990; Restrepo *et al.* 1993;

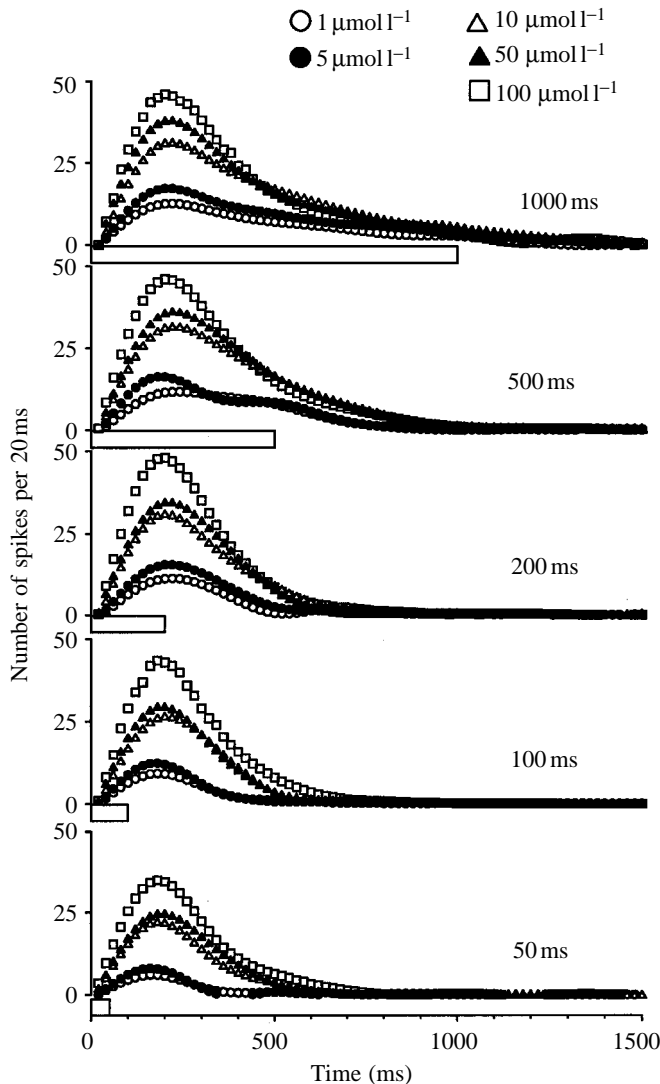


Fig. 8. Population responses to different odor step amplitudes at the same step length. Responses of all 14 receptor cells were summed and smoothed as in Fig. 7. Odor step lengths are indicated by the open box along the x -axis.

Boekhoff *et al.* 1994) have shown that, in both vertebrates and invertebrates, second messenger concentrations peak within 50 ms and decline to baseline levels within 250 ms following exposure to odorants. However, different species have shown a range of temporal capabilities in the stimulus-response kinetics of their olfactory receptor cells. Although the studies are relatively sparse, it seems that invertebrates employ faster kinetic processes than vertebrates. Dethier (1968) demonstrated that the blowfly (*Phormia regina*) can behaviorally discriminate stimulus intensity within the first 100 ms of the responses generated by tarsal receptor cells; the receptor cells show most of the intensity information in the first 500 ms (Smith *et al.* 1983). Moth (*Bombyx mori*) pheromone receptors, at high stimulus load, respond with a phasic spike burst that terminates within 250 ms (Kaissling, 1986). In addition, studies using pulsatile stimuli have shown that heliothine moth pheromone receptors can encode repetition

rates up to 12 Hz (Almaas *et al.* 1991). Receptor potential generation in spiny lobster *Panulirus argus* olfactory receptor neurons also follows a rapid time course, generating excitatory currents as fast as 20 ms following stimulation (Fadool *et al.* 1993) and peaking after 350 ms (Schmiedel-Jakob *et al.* 1989).

Vertebrate chemoreceptors have been shown to follow a slightly slower time course. Studies on salamander (*Ambystoma tigrinum*) olfactory receptor neurons showed that channel gating kinetics (Zufall *et al.* 1993), receptor potential generation (Firestein and Werblin, 1989; Kurahashi, 1989; Kurahashi and Shibuya, 1990) and spike activity (Kauer and Shepherd, 1975; Getchell and Shepherd, 1978) peak after several hundred milliseconds following the onset of an odor pulse. Firestein *et al.* (1990, 1993) measured an integration time of over 1 s for these receptor cells. Thus, since the 50 ms time course of second messenger production of both vertebrates and invertebrates is rather consistent among different species, while receptor potential generation is more variable, it appears that the temporal properties of chemoreceptor cells such as integration time may be determined at the level of receptor potential generation. Kelling and Halpern (1983) have shown in human psychophysical experiments that 100 ms stimulus pulses on the tongue may be adequate to determine stimulus quality, but longer pulses (several hundred milliseconds) are required to determine stimulus intensity.

The spike responses generated by the Hyp receptor cells tested in this study demonstrated the rapid kinetics of lobster olfactory receptor cells. Spike responses were often phasic, integrating stimulus events occurring in the first 200 ms following odor step onset. This integration time of 200 ms (Figs 4, 7) and the time window of approximately 100–300 ms for stimulus intensity discrimination (Fig. 8) suggests that these receptor cells encode stimulus events at the 100 ms time scale. This has important implications regarding the filtering of odor signals. In natural odor plumes, odor concentrations will be perceived to fluctuate slowly when integrated over a long period or will appear to fluctuate more rapidly when integrated over a shorter period (Murlis, 1986; Moore and Atema, 1988); thus, integration time plays an important role in the perception of the dynamic features of odor plumes. The shortest odor pulses that have been measured in turbulent plumes in water are of the order of approximately 0.5 s (Moore *et al.* 1992). However, studies on natural odor plumes are still sparse; thus, the full spectrum of odor pulse parameters is still unknown. The pulse lengths measured thus far are well within the range of detection of lobster Hyp receptors. The 100 ms time scale of lobster chemoreceptor filters sets constraints on the features of an odor plume that are available to an orienting lobster.

It is interesting to note that the 200 ms integration time of the Hyp chemoreceptor cells is closely matched to the lobster's olfactory sampling behavior. Lobsters periodically flick their lateral antennules, resulting in a reduced boundary layer thickness surrounding the aesthetasc tufts (Moore *et al.* 1991a). Flicking enhances olfactory stimulation (Schmitt and Ache,

1979; Gleeson *et al.* 1993). The downstroke of the flick takes 80–100 ms (Moore and Atema, 1988; J. Atema, personal observation) and lobsters may flick as rapidly as 4–5 times per second (Berg *et al.* 1992; Leonard *et al.* 1994). The 200 ms time frame of olfactory intensity discrimination as determined in this physiological study may have evolutionarily constrained the rate of this olfactory sampling behavior: the lobster obtains a single sample, determines the concentration of the sample within 200 ms and can obtain a new sample with the next flick.

The Hyp receptor cells used in this study showed rapid adaptation (Fig. 8). Although decreased odor step amplitude resulted in a delay in first spike latency as well as an increased variance in the latency (Fig. 6), there was no effect on the latency of the peak response (Fig. 8). The effects of adaptation were prominent after approximately 300 ms: immediately following the peak in spike activity, the receptor cell response began to decline towards baseline. Adaptation is an important mechanism for lobster chemoreceptors to act as temporal filters (Atema, 1985). The filter bandwidth for the cells studied appeared to be rather narrowly focused around 5 Hz. This corresponds to the observation that some lobster Hyp-sensitive cells can follow stimulus pulses as rapidly as 4 Hz (Gomez *et al.* 1994).

It is likely that different adaptation processes with different time courses are involved. Slower adaptation processes allow the system to reset sensitivity in a 'noisy' (i.e. chemical background) environment (Borroni and Atema, 1988). Various forms of adaptation may thus allow the lobster's chemoreceptor system to function continuously in naturally pulsatile odor plumes (Atema, 1987). The moth receptor cells' capability to encode 10 Hz pulse trains reflects their behavioral response to strands of odor in a turbulent pheromone plume (Baker, 1990; Murlis *et al.* 1992).

In addition to responding to stimulus onsets, some chemoreceptors have been shown to respond to the removal of a stimulus. Salamander (*Ambystoma tigrinum*) olfactory receptor neurons (Kauer and Shepherd, 1975; Getchell and Shepherd, 1978) and moth (*Bombyx mori*) pheromone receptor cells (Kaissling, 1986) respond to an odor offset with a brief cessation of tonic spike activity or a transient hyperpolarization. In addition, Kurahashi *et al.* (1994) also demonstrated depolarizing responses to odor offsets in isolated salamander olfactory receptor cells. The chemoreceptors in this study and in other related studies (Voigt and Atema, 1988; Gomez *et al.* 1994) generally did not show a response to odor offsets. Lobster chemoreceptors may thus be optimized to detect only stimulus onsets. Moore and Atema (1988, 1991) showed that pulse onset slopes provide among the strongest spatial gradients found in turbulent odor plumes. Thus, receptor cells that are specialized to detect a variety of odor onset slopes may best be suited to extract onset slope gradients from odor plumes. The temporal properties of lobster Hyp receptor cells found in this study support the hypothesis that these chemoreceptors may aid in the filtering of distance information from the fine structure in turbulent odor plumes.

The authors would like to thank Dr Rainer Voigt for his invaluable technical assistance and critical reading of the

manuscript. This work was supported by NSF IBN 9222774 to J.A. and was part of the dissertation research of G.G.

References

- ALMAAS, T. J., CHRISTENSEN, T. A. AND MUSTAPARTA, H. (1991). Chemical communication in heliothine moths. I. Antennal receptor neurons encode several features of intra- and interspecific odorants in the male corn earworm moths *Helicoverpa zea*. *J. comp. Physiol. A* **169**, 249–258.
- ATEMA, J. (1985). Chemoreception in the sea: adaptation of chemoreceptors and behavior to aquatic stimulus conditions. *Soc. exp. Biol. Symp.* **39**, 387–423.
- ATEMA, J. (1987). Aquatic and terrestrial chemoreceptor organs: morphological and physiological designs for interfacing with chemical stimuli. In *Comparative Physiology: Life in Water and on Land* (ed. P. Dejours, L. Bolis, C. R. Taylor and E. R. Weibel), pp. 303–316. Padova: IX-Liviana Press.
- ATEMA, J. (1988). Distribution of chemical stimuli. In *Sensory Biology of Aquatic Animals* (ed. J. Atema, R. R. Fay, A. N. Popper and W. N. Travalga), pp. 29–56. New York: Springer-Verlag.
- BAKER, T. C. (1990). Upwind flight and casting flight: complementary phasic and tonic systems used for location of sex pheromone sources by male moths. In *Proceedings of the Tenth International Symposium on Olfaction and Taste* (ed. K. B. Døving), pp. 18–25. Oslo: Graphic Communication Systems A/S.
- BARLOW, H. B. (1958). Temporal and spatial summation in human vision at different background intensities. *J. Physiol., Lond.* **141**, 337–350.
- BASIL, J. A., GRASSO, F. AND ATEMA, J. (1995). High resolution odor measurement from freely moving lobsters in turbulent odor plumes. *Chem. Senses* **20**, 664.
- BERG, K., VOIGT, R. AND ATEMA, J. (1992). Flicking in the lobster *Homarus americanus*: recordings from electrodes implanted in antennular segments. *Biol. Bull. mar. biol. Lab., Woods Hole* **183**, 377–378.
- BOEKHOFF, I., MICHEL, W. C., BREER, H. AND ACHE, B. W. (1994). Single odors differentially stimulate dual second messenger pathways in lobster olfactory receptor cells. *J. Neurosci.* **14**, 3304–3309.
- BORRONI, P. F. AND ATEMA, J. (1988). Adaptation in chemoreceptor cells. I. Self-adapting backgrounds determine threshold and cause parallel shift of response function. *J. comp. Physiol. A* **164**, 64–74.
- BREER, H., BOEKHOFF, I. AND TAREILUS, E. (1990). Rapid kinetics of second messenger formation in olfactory transduction. *Nature* **345**, 65–68.
- DETHIER, V. G. (1968). Chemosensory input and taste discrimination in the blowfly. *Science* **161**, 389–391.
- DEVINE, D. V. AND ATEMA, J. (1982). Function of chemoreceptor organs in spatial orientation of the lobster *Homarus americanus*: differences and overlap. *Biol. Bull. mar. biol. Lab., Woods Hole* **163**, 144–153.
- DUYSENS, J., GULYAS, B. AND MAES, H. (1991). Temporal integration in cat visual cortex: a test of Bloch's law. *Vision Res.* **31**, 1517–1528.
- FADOOL, D. A., MICHEL, W. C. AND ACHE, B. W. (1993). Odor sensitivity of cultured lobster olfactory receptor neurons is not dependent on process formation. *J. exp. Biol.* **174**, 215–233.
- FIRESTEIN, S., PICCO, C. AND MENINI, A. (1993). The relationship between stimulus and response in olfactory receptor cells of the tiger salamander. *J. Physiol., Lond.* **469**, 1–10.
- FIRESTEIN, S., SHEPHERD, G. M. AND WERBLIN, F. S. (1990). Time

- course of the membrane current underlying sensory transduction in salamander olfactory receptor neurones. *J. Physiol., Lond.* **430**, 135–158.
- FIRESTEIN, S. AND WERBLIN, F. (1989). Odor-induced membrane currents in vertebrate olfactory receptor neurons. *Science* **244**, 79–82.
- GERHARDT, G. A., OKE, A. F. AND G. NAGY, G. (1982). Nafion coated electrodes with high selectivity for CNS electrochemistry. *Brain Res.* **290**, 390–395.
- GETCHELL, T. V. AND SHEPHERD, G. M. (1978). Responses of olfactory receptor cells to step pulses odour at different concentrations in the salamander. *J. Physiol., Lond.* **282**, 521–540.
- GLEESON, R. A., CARR, W. E. S. AND TRAPIDO-ROSENTHAL, H. G. (1993). Morphological characteristics facilitating stimulus access and removal in the olfactory organ of the spiny lobster, *Panulirus argus*: insight from the design. *Chem. Senses* **18**, 67–75.
- GOMEZ, G., VOIGT, R. AND ATEMA, J. (1992). High resolution measurement and control of chemical stimuli in the lateral antennule of the lobster *Homarus americanus*. *Biol. Bull. mar. biol. Lab., Woods Hole* **183**, 353–354.
- GOMEZ, G., VOIGT, R. AND ATEMA, J. (1994). Frequency filter properties of lobster chemoreceptor cells determined with high-resolution stimulus measurement. *J. comp. Physiol. A* **174**, 803–811.
- HOOD, D. C. AND GROVER, B. G. (1974). Temporal summation of light by a vertebrate visual receptor. *Science* **184**, 1003–1005.
- JOHNSON, B. R. AND ATEMA, J. (1983). Narrow-spectrum chemoreceptor cells in the antennules of the American lobster, *Homarus americanus*. *Neurosci. Lett.* **41**, 145–150.
- JOHNSON, B. R., VOIGT, R., MERRILL, C. L. AND ATEMA, J. (1991). Across-fiber patterns may contain a sensory code for stimulus intensity. *Brain Res. Bull.* **26**, 327–331.
- KAISLING, K.-E. (1986). Temporal characteristics of pheromone receptor cell responses in relation to orientation behaviour of moths. In *Mechanisms in Insect Olfaction* (ed. T. L. Payne, M. C. Birch and C. E. J. Kennedy), pp. 193–199. Oxford: Oxford University Press.
- KAISLING, K.-E. AND KRAMER, E. (1990). Sensory basis of pheromone-mediated orientation in moths. *Verh. dt. zool. Ges.* **83**, 109–131.
- KAUER, J. AND SHEPHERD, G. M. (1975). Olfactory stimulation with controlled and monitored step pulses of odor. *Brain Res.* **85**, 108–113.
- KELLING, S. T. AND HALPERN, B. P. (1983). Taste flashes: reaction times, intensity and quality. *Science* **219**, 412–414.
- KURAHASHI, T. (1989). Activation by odorants of cation-selective conductance in the olfactory receptor cell isolated from the newt. *J. Physiol., Lond.* **419**, 177–192.
- KURAHASHI, T., LOWE, G. AND GOLD, G. H. (1994). Suppression of odorant responses by odorants in olfactory receptor cells. *Science* **265**, 118–120.
- KURAHASHI, T. AND SHIBUYA, T. (1990). Ca^{2+} -dependent adaptive properties in the solitary olfactory receptor cell of the newt. *Brain Res.* **515**, 261–268.
- LAING, D. G. AND MACLEOD, P. (1992). Reaction time for the recognition of odor quality. *Chem. Senses* **17**, 337–346.
- LEONARD, A. E., VOIGT, R. AND ATEMA, J. (1994). Lobster orientation in turbulent odor plumes: electrical recording of bilateral olfactory sampling (antennular “flicking”). *Biol. Bull. mar. biol. Lab., Woods Hole* **187**, 273.
- LESTER, B. AND HALPERN, B. P. (1979). Effect of stimulus presentation duration on gustatory reaction time. *Physiol. Behav.* **22**, 319–324.
- LEVICK, W. R. AND ZACKS, J. L. (1970). Responses of cat retinal ganglion cells to brief flashes of light. *J. Physiol., Lond.* **206**, 677–700.
- MAFRA-NETO, A. AND CARDÉ, R. T. (1994). Fine-scale structure of pheromone plumes modulates upwind orientation of flying moths. *Nature* **369**, 142–144.
- MOORE, P. A. AND ATEMA, J. (1988). A model of a temporal filter in chemoreception to extract directional information from a turbulent odor plume. *Biol. Bull. mar. biol. Lab., Woods Hole* **17**, 355–363.
- MOORE, P. A. AND ATEMA, J. (1991). Spatial information in a three-dimensional fine structure of an aquatic odor plume. *Biol. Bull. mar. biol. Lab., Woods Hole* **181**, 408–418.
- MOORE, P. A., ATEMA, J. AND GERHARDT, G. A. (1991a). Fluid dynamics and microscale chemical movement in the chemosensory appendages of the lobster, *Homarus americanus*. *Chem. Senses* **16**, 663–674.
- MOORE, P. A., SCHOLZ, N. AND ATEMA, J. (1991b). Chemical orientation of lobsters, *Homarus americanus*, in turbulent odor plumes. *J. chem. Ecol.* **17**, 1293–1307.
- MOORE, P. A., ZIMMER-FAUST, R., BEMENT, S., WEISSBURG, M., PARRISH, J. AND GERHARDT, G. (1992). Measurement of microscale patchiness in a turbulent aquatic odor plume using a semiconductor-based microprobe. *Biol. Bull. mar. biol. Lab., Woods Hole* **183**, 138–142.
- MURLIS, J. (1986). The structure of odor plumes. In *Mechanisms in Insect Olfaction* (ed. T. L. Payne, M. C. Birch and C. E. J. Kennedy), pp. 27–38. Oxford: Oxford University Press.
- MURLIS, J., ELKINTON, J. S. AND CARDÉ, R. T. (1992). Odor plumes and how insects use them. *A. Rev. Ent.* **37**, 505–532.
- RESTREPO, D., BOEKHOFF, I. AND BREER, H. (1993). Rapid kinetic measurements of second messenger formation in olfactory cilia from channel catfish. *Am. J. Physiol.* **264**, 906–911.
- SCHMIEDEL-JAKOB, I., ANDERSON, P. A. V. AND ACHE, B. W. (1989). Whole cell recording from lobster olfactory receptor cells: responses to current and odor stimulation. *J. Neurophysiol.* **61**, 994–1000.
- SCHMITT, B. C. AND ACHE, B. W. (1979). Olfaction: responses of a decapod crustacean are enhanced by flicking. *Science* **205**, 204–206.
- SMITH, D. V., BOWDAN, E. AND DETHIER, V. G. (1983). Information transmission in tarsal sugar receptors of the blowfly. *Chem. Senses* **8**, 81–101.
- SOKAL, R. R. AND ROHLF, F. J. (1981). *Biometry*, 2nd edn. New York: W. H. Freeman and Co.
- VICKERS, N. J. AND BAKER, T. C. (1994). Reiterative responses to single strands of odor promote sustained upwind flight and odor source location by moths. *Proc. natn. Acad. Sci. U.S.A.* **91**, 5756–5760.
- VOIGT, R. AND ATEMA, J. (1988). Effects of stimulus profile on temporal response profile and disadaptation time course. *Chem. Senses* **13**, 742.
- WEISSBURG, M. J. AND ZIMMER-FAUST, R. K. (1993). Life and death in moving fluids: hydrodynamic effects on chemosensory-mediated predation. *Ecology* **74**, 1428–1443.
- ZIMMER-FAUST, R. K., FINELLI, C. M., PENTCHEFF, N. D. AND WETHEY, D. S. (1995). Odor plumes and animal navigation in turbulent water flow: A field study. *Biol. Bull. mar. biol. Lab., Woods Hole* **188**, 111–116.
- ZUFALL, F., HATT, H. AND FIRESTEIN, S. (1993). Rapid application and removal of second messengers to cyclic nucleotide-gated channels from olfactory epithelium. *Proc. natn. Acad. Sci. U.S.A.* **90**, 9335–9339.